Journal of Engineering Mathematics, Vol. 12, No. 4, October 1978
Sijthoff & Noordhoff International Publishers–Alphen aan den Rijn
Printed in The Netherlands

Tensile deformation of a round bar

P. P. GILLIS and S. E. JONES

College of Engineering, University of Kentucky, Lexington, Kentucky 40506, *USA*

(Received January 17, 1978)

SUMMARY

An approximate mathematical description of the tensile test is given for a material that is strain hardening and strain rate sensitive. Three phases of the deformation are distinguished: (I) nearly homogeneous deformation up to maximum load, (II) gradual localization of the deformation at nearly constant load, and (III) necking. The analysis realistically approximates: load, extension curves; post-uniform elongation; incipient neck size; and neck profiles.

1. Introduction

In recent years there have been dramatic advances in the technology of sheet metal forming and in the analysis of such problems. As examples, consider superplastic or creep forming of titanium, and the mapping of formability limit diagrams. These developments, in turn, have led to increased efforts to understand plastic instability—the process that most often limits formability. Necking of a ductile tension specimen prior to fracture is probably the most familiar example of plastic instability. It also seems to be the simplest situation in which strain localization occurs. Consequently, much of the recent work on plastic instability relates to the tension test.

The classic treatment of the phenomenon now known as plastic instability was published by Considere [1] in 1885. However, Considere's result is only applicable to strain rate insensitive materials. In the early 1960's American attention became focussed on the dramatic suppressions of plastic instability that could occur in strongly rate-sensitive materials. Backofen, Turner and Avery [2] were among the first to attempt to quantify the effect of strain rate sensitivity.

Subsequently, Hart [3] developed a more general, unified analysis of the tension test. In Hart's analysis the material constitutive relation includes strain hardening and strain rate sensitivity. Plastic stability is defined in terms of the hardening and rate-sensitivity parameters of the constitutive relation and plastic instability is defined as any violation of the criterion for stability. Hart does recognize, however, that instability in this sense need not be catastrophic but could proceed to localize the plastic deformation at a very slow rate. Shortly afterwards, Campbell [4] also put forward a theory of plastic instability in rate-sensitive materials. Campbell structured his analysis in terms of an axial strain gradient in the specimen. Most subsequent analyses of the problem have used Hart's analysis, or Campbell's, or both as starting points. See, for example, Jonas and co-workers [5, 6]. Later, Argon [7] introduced a more general material constitutive relation into the problem.

Hutchinson and Obrecht [8] made an important conceptual advance. They adopt the

Hart approach of comparing two cross sections of different areas but abandoned the Hart criterion for stability. Instead, they calculated the strain history in the larger cross section up to the time to failure of the smaller. Hutchinson and Neale [9] refined this concept to define the critical state for necking as being when the largest cross section ceases to deform. However, calculations by Ghosh [10] indicate that in rate-sensitive materials pronounced necking is suppressed until long after the largest cross section stops deforming. Ghosh himself defines tensile deformation as being stable so long as it is accompanied by a load rise [11]. Despite their differences, both Ghosh and Hutchinson conclude that material strain rate sensitivity can lead to significant delay in necking.

In the present paper, the effect of strain rate sensitivity on the tensile deformation of a round bar is assessed. The general approach is that of Hart [3] but the criterion for plastic instability is the formation of a neck, that is, severe localization of the deformation. In a rate-insensitive material a neck can form immediately upon reaching the maximum load. However, this cannot occur in a rate-sensitive material because deformation localization would increase the strain rate and, therefore, the stress at the neck which would increase the load. Instead, the deformation proceeds through a stage of steadily increasing non-homogeneity. The increase of strain rate is compensated by a decrease of cross sectional area to prevent the load from rising. Finally, the deformation becomes sufficiently localized that a distinct neck forms and the load drops rapidly.

An approximate analysis of this process is developed in terms of three distinct phases: (I) nearly homogeneous deformation up to maximum load, (II) gradual localization of the deformation at constant load, and (III) necking. Pieced together these form a realistic approximation to actual load, extension curves for round tensile specimens of rate sensitive materials.

2. Material

We consider a material whose behavior is governed by a relation of the form:

$$\Delta\dot{\varepsilon}/\dot{\varepsilon} = N\Delta\sigma/\sigma - G\Delta\varepsilon \tag{1.1}$$

where the stress, σ, strain, ε, and strain rate, $\dot{\varepsilon}$, are defined in the next section. The symbol Δ denotes change in the indicated variable. That change can be in space or time and can be finite. Furthermore, the functions N and G are experimentally determined and in general will depend upon σ, $\dot{\varepsilon}$, $\Delta\sigma$, $\Delta\varepsilon$, and $\Delta\dot{\varepsilon}$. Under quasi-static loading, temperature changes caused by adiabatic heating are not considered to be significant and are, therefore, omitted in the determination of N and G. Strain is also omitted. For, although the state of the material changes with strain, the state is not measured by the strain, as shown by Hart [12].

A strain hardening parameter is now defined as $\gamma \equiv G/N$, which is obviously a function of all the variables listed above. Similarly, a strain rate sensitivity parameter is defined as $\nu \equiv 1/N$. In terms of these parameters equation (1.1) can be recast as

$$\Delta\sigma/\sigma = \gamma\Delta\varepsilon + \nu\Delta\dot{\varepsilon}/\dot{\varepsilon} \tag{1.2}$$

which is assumed to describe the material response to tensile deformation.

3. Phase I

The initial deformation stage consists of relatively homogeneous straining up to the maximum load. However, the presence of initial variations in specimen cross section leads to relatively small inhomogeneities in the deformation. The analysis of this phase consists of comparing two different cross sections of the bar at some fixed time during the deformation.

Let the initial cross sectional area of one cross section be denoted by A_0 and let A be the area of this section under some load P less than the maximum load P_H. The strain measure to be employed is defined by

$$\varepsilon \equiv \ln(A_0/A) \tag{2.1}$$

which agrees quite accurately with the usual notion of axial strain when the deformation is isochoric. The corresponding measure of strain rate is

$$\dot{\varepsilon} = -\dot{A}/A \tag{2.2}$$

where the superposed dot denotes differentiation with respect to time. The stress measure to be employed is the mean section stress defined by

$$\sigma \equiv P/A \tag{2.3}$$

which, as the most convenient quantity, is the stress measure most often used in actual practice.

Let the initial area of another cross section be denoted by $A_0 + \Delta A_0 = A_0(1 + \Delta A_0/A_0)$ and let $A + \Delta A = A(1 + \Delta A/A)$ be the area of this section under the load P. We denote the strain of this cross section as $\varepsilon + \Delta\varepsilon$ and by analogy with (2.1)

$$\varepsilon + \Delta\varepsilon = \ln[A_0(1 + \Delta A_0/A_0)/A(1 + \Delta A/A)]. \tag{2.4}$$

Thus, the difference in strains between the two cross sections is

$$\Delta\varepsilon = \ln[(1 + \Delta A_0/A_0)/(1 + \Delta A/A)]. \tag{2.5}$$

Differentiation of (2.5) with respect to time gives

$$\Delta\dot{\varepsilon} = \frac{\dot{A}\Delta A/A^2 - \Delta\dot{A}/A}{1 + \Delta A/A} = \frac{-(\dot{A}/A)(\Delta\dot{A}/\dot{A} - \Delta A/A)}{1 + \Delta A/A}, \tag{2.6}$$

so that

$$\Delta\dot{\varepsilon}/\dot{\varepsilon} = (\Delta\dot{A}/\dot{A} - \Delta A/A)/(1 + \Delta A/A). \tag{2.7}$$

The stress at this second cross section is denoted by $\sigma + \Delta\sigma = \sigma(1 + \Delta\sigma/\sigma)$ and equals $P/[A(1 + \Delta A/A)]$ where the load P is the same as at the first cross section, as given by equation (2.3). Consequently, $(1 + \Delta\sigma/\sigma)(1 + \Delta A/A) = 1$ and

$$\Delta\sigma/\sigma = -(\Delta A/A)/(1 + \Delta A/A) \tag{2.8}$$

describes the relative stress difference between the two arbitrary cross sections.

Substitution of the kinematic expressions in (2.5) and (2.7) and the equilibrium requirement (2.8) into (1.2) gives

$$\frac{-\Delta A/A}{1+\Delta A/A}=\gamma\ln\left[\frac{1+\Delta A_0/A_0}{1+\Delta A/A}\right]+\nu\left[\frac{\Delta\dot{A}/\dot{A}-\Delta A/A}{1+\Delta A/A}\right]. \tag{2.9}$$

Rearranging equation (2.9) and solving for $\Delta\dot{A}/\dot{A}$ gives

$$\nu(\Delta\dot{A}/\dot{A})=(\nu-1)(\Delta A/A)-\gamma(1+\Delta A/A)\ln[(1+\Delta A_0/A_0)/(1+\Delta A/A)]. \tag{2.10}$$

Equation (2.10) shows that the two arbitrary cross sections under consideration will in general be deforming at different rates ($\Delta\dot{A}\neq 0$). Only for the case $\Delta A_0=0$ can equation (2.10) admit of a solution $\Delta\dot{A}=0$ when $\Delta A=0$. Consequently, either a nonuniform strain rate distribution exists in the specimen during this phase of deformation, or a nonuniform strain distribution exists, or both. Thus, we arrive at maximum load with a spatial variation in ε and $\dot{\varepsilon}$ along the specimen.

The condition for the occurrence of maximum load is given by equation (2.10) interpreted somewhat differently than in the paragraph above. Imagine comparing section A at some time t, with itself at some later time $t+\Delta t>t$. Then if we require that as $\Delta t\rightarrow 0$ the load P at $t+\Delta t$ be the same as the load at t, i.e., $dP/dt=0$ at t, the algebra of the analysis is almost exactly the same as the previous development. The differences are that certain Δ quantities become d quantities as Δt is made small and we may, without loss of generality, choose a cross section for which $\Delta A_0=0$. Since $(1+dA/A)$ is close to unity its logarithm is dA/A and from (2.10) the condition for maximum load is

$$\nu d\dot{A}/\dot{A}=(\nu-1)dA/A-\gamma(1+dA/A)dA/A \tag{2.11}$$

where the term dA/A can be neglected in comparison to unity in the coefficient of γ. Thus, the maximum load criterion is

$$\gamma=1-\nu-(\nu/\dot{\varepsilon})(d\dot{A}/dA) \tag{2.12}$$

which approximates Hart's criterion, $\gamma=1-\nu$, whenever $|d\dot{A}/dA|\ll\dot{\varepsilon}$ and is certainly Considere's criterion, $\gamma=1$, when $\nu=0$.

4. Phase II

This phase is characterized approximately by a period of constant load and gradual concentration of the deformation into the vicinity of that cross section which is straining fastest at the beginning of this phase. In this section of the analysis we need consider only that one cross section which we call the critical cross section. We let the subscript H denote conditions at the critical section at the maximum load.

As the strain at this section increases from ε_H to ε the cross sectional area decreases from $A_0\exp\{-\varepsilon_H\}$ to $A_0\exp\{-\varepsilon\}$. For the load to remain constant:

$$P/P_H=1 \tag{3.1}$$

the stress here must increase from σ_H to $\sigma=\sigma_H\exp\{\varepsilon-\varepsilon_H\}$.

Now the increments in stress, strain and strain rate in going from the reference state at time t_H to a later state at time $t > t_H$ are

$$\Delta\sigma/\sigma = (\sigma - \sigma_H)/\sigma_H = \sigma/\sigma_H - 1 = \exp\{\varepsilon - \varepsilon_H\} - 1, \tag{3.2}$$

$$\Delta\varepsilon = \varepsilon - \varepsilon_H, \tag{3.3}$$

$$\Delta\dot{\varepsilon}/\dot{\varepsilon} = (\dot{\varepsilon} - \dot{\varepsilon}_H)/\dot{\varepsilon}_H = \dot{\varepsilon}/\dot{\varepsilon}_H - 1. \tag{3.4}$$

Rearranging the material relation (1.2) and using (3.2)–(3.4) gives

$$v\dot{\varepsilon}/\dot{\varepsilon}_H = \exp\{\varepsilon - \varepsilon_H\} - 1 - \gamma(\varepsilon - \varepsilon_H) + v \tag{3.5}$$

so that

$$v\,d\varepsilon/dt = \dot{\varepsilon}_H[\exp\{\varepsilon - \varepsilon_H\} - 1 - \gamma(\varepsilon - \varepsilon_H) + v] \tag{3.6}$$

which can be integrated to obtain t as a function of ε. For a test at constant crosshead speed, S, we can accurately approximate $\dot{\varepsilon}_H$ by $S/L_H = (S/L_0)\exp\{-\varepsilon_H\}$ where L_0 is the initial length of the specimen. Thus:

$$(S/L_0)(t - t_H) = \int_{\varepsilon_H}^{\varepsilon} \frac{v\exp\{\varepsilon_H\}\,d\varepsilon}{\exp\{\varepsilon - \varepsilon_H\} - 1 - \gamma(\varepsilon - \varepsilon_H) + v}. \tag{3.7}$$

With the time expressed as a function of the critical strain it is quite simple to calculate the nominal or engineering strain, $e = (L/L_0 - 1)$, based upon the incorrect assumption of homogeneous deformation. For constant crosshead speed $L = L_0 + St = L_H + S(t - t_H)$ so that

$$e = \exp\{\varepsilon_H\} + (S/L_0)(t - t_H) - 1 \tag{3.8}$$

where $(S/L_0)(t - t_H)$ is obtained from equation (3.7) above.

This phase of the deformation proceeds with increasing strain rate at the critical cross section, according to equation (3.6), until the deformation is focussed intensely enough that a neck forms here and the load subsequently decreases.

5. Phase III

The analysis of this phase of the deformation first assumes the existence of a well developed neck centered at the critical cross section. After the neck is analysed its severity is reduced until stress, strain and strain rate can be matched with conditions in Phase II. At this point the deformation mode changes from localizing under nearly constant load to necking under rapidly decreasing load.

Analysis of the well developed neck is based upon the existence of an empirical description of the neck shape, say

$$r(x, t) = f(a(t), x) \tag{4.1}$$

where r is the specimen radius an axial distance x away from the critical section and a is the radius of the critical section. Alternatively, the cross sectional areas can be prescribed:

$$A(x, t) = F(\varepsilon_n(t), x) \tag{4.2}$$

where ε_n is the strain at the critical section.

Differentiation of equation (4.2) with respect to time gives a relation of the form:

$$\dot{A}(x) = (\partial F/\partial \varepsilon_n)\dot{\varepsilon}_n \tag{4.3}$$

and for realistically prescribed shapes there will be some value of x, say X, for which $\dot{A}$ equals zero. This value, X, defines the extent of the deforming zone, or neck, at prescribed ε_n and t. For $|x| > |X|$ no deformation occurs as it is physically unreasonable for $\dot{A}$ to be positive.

From equations (2.2), (4.2) and (4.3) we have

$$\dot{\varepsilon}(x) = \begin{cases} -\dot{\varepsilon}_n(\partial F/\partial \varepsilon_n)/F, & |x| < |X|, \\ 0, & |x| \geq |X|. \end{cases} \tag{4.4}$$

Then, as all deformation is taking place within $-X < x < X$ and this deformation is symmetrical about $x = 0$, we can write

$$S = 2\int_0^{X(\varepsilon_n)} \dot{\varepsilon}(x)\,dx. \tag{4.5}$$

Upon noting that $\dot{\varepsilon}_n$ is independent of x, equation (4.5) gives

$$\dot{\varepsilon}_n = -S\Big/\left(2\int_0^{X(\varepsilon_n)} [(\partial F/\partial \varepsilon_n)/F]\,dx\right) \tag{4.6}$$

as the strain rate in the critical cross section. As was the case during Phase II, this strain rate equation can be integrated to give the time as a function of necking strain. Let subscript J refer to conditions at the transition from localizing (Phase II) to necking (Phase III). Then

$$(S/L_0)(t - t_J) = 2\int_{\varepsilon_J}^{\varepsilon_n}\left[\int_0^{X(\varepsilon_n)} [(\partial F/\partial \varepsilon_n)/F]\,dx\right]d\varepsilon_n. \tag{4.7}$$

The value of ε_J is that for which $\dot{\varepsilon}_n$, equation (4.6), equals $\dot{\varepsilon}$ as given by equation (3.6).

As during the previous phase the nominal strain can be calculated:

$$e = \exp\{\varepsilon_J\} + (S/L_0)(t - t_J) - 1. \tag{4.8}$$

Applying the material relation (1.2) as before we have

$$\Delta\sigma/\sigma = (\sigma_n - \sigma_H)/\sigma_H = \sigma_n/\sigma_H - 1, \tag{4.9}$$

$$\Delta\varepsilon = \varepsilon_n - \varepsilon_H, \tag{4.10}$$

$$\Delta\dot{\varepsilon}/\dot{\varepsilon} = (\dot{\varepsilon}_n - \dot{\varepsilon}_H)/\dot{\varepsilon}_H = \dot{\varepsilon}_n/\dot{\varepsilon}_H - 1 = -(L_0/2)\exp\{\varepsilon_H\}\int_0^{X(\varepsilon_n)} [(\partial F/\partial\varepsilon_n)/F]dx - 1. \quad (4.11)$$

The decreasing load is $P = \sigma_n A_0 \exp\{\varepsilon_n\}$ whereas the formerly constant load is $P_H = \sigma_H A_0 \exp\{\varepsilon_H\}$. Consequently

$$P/P_H = (\sigma_n/\sigma_H)\exp\{\varepsilon_n - \varepsilon_H\} \quad (4.12)$$

which from the material relation is

$$P/P_H = \left[1 + \gamma(\varepsilon_n - \varepsilon_H) - (\nu L_0/2)\exp\{\varepsilon_H\}\int_0^{X(\varepsilon_n)} [(\partial F/\partial\varepsilon_n)/F]dx - \nu\right]\exp\{\varepsilon_H - \varepsilon_n\}. \quad (4.13)$$

From the equation sets (3.1), (3.7), (3.8) and (4.13), (4.7), (4.8), the entire load (ratio) vs nominal strain (essentially, time, but in more convenient units) can be determined as a function of the parameters ε and ε_n (which are actually the same, only ε refers to Phase II deformation and ε_n to Phase III) for all strains (times) in the critical section greater than ε_H $(t > t_H)$.

In the following section the details of this procedure are presented for a particular form of the function $A(x, t) = F(\varepsilon_n(t), x)$.

6. Example

Neck Kinematics

Neck profile equations of the type (4.1) have been published by Dondik [13] and by Argon et al. [14] which empirically describe actual profile measurements to a high degree of accuracy. An equally empirical but somewhat more directly interpretable relation is used here as the basis for an example calculation. In the form of equation (4.2) this relation is

$$A = \pi(a_0/k\varepsilon_n)^2\exp\{-\varepsilon_n\}(1 + k\varepsilon_n - [1 - (xk\varepsilon_n/a_0)^2\exp\{-\varepsilon_n\}]^{\frac{1}{2}})^2. \quad (5.1)$$

Here a_0 is the initial radius of the bar, k is a constant equal to 0.75, ε_n is the strain at the neck, x is current axial distance from the neck and A is the cross sectional area at x. In this form it is no easier to interpret than those cited above.

Equation (5.1) derives from the observation by Bridgman [15] that the radius of curvature of a tensile neck in a round bar can be accurately correlated with neck strain. Figure 1 shows Bridgman's correlation for several materials over a wide range of neck strains. For the range $0.2 \leq \varepsilon_n \leq 2.0$ the linear relation

$$a/R = k\varepsilon_n \quad (5.2)$$

where $k = 0.75$, shown as a dashed line in the figure, is an accurate representation of the trend of the data. We use (5.2) as the description of the geometry of the neck.

Rather than proceed by using (5.1), which derives simply from (5.2), and the formal mathematical development of Section 4, the elements of the Phase III analysis can be made

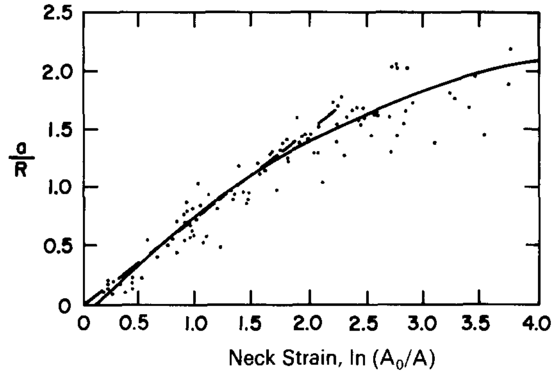

Figure 1. Ratio of specimen radius to radius of curvature at a neck versus strain at the neck for several different materials. Taken from Bridgman, Reference 15.

clearer by employing (5.2) directly. Figure 2 shows the neck geometry. Using the Pythagorean theorem we have

$$R^2 = x^2 + (R + a - r)^2, \tag{5.3}$$

from which

$$r = R + a - [R^2 - x^2]^{\frac{1}{2}}. \tag{5.4}$$

Differentiation of (5.4) with respect to time yields

$$\dot{r} = \dot{R} + \dot{a} - R\dot{R}[R^2 - x^2]^{-\frac{1}{2}}. \tag{5.5}$$

Differentiation of (5.2) with respect to time yields

$$\dot{a}/R - a\dot{R}/R^2 = k\dot{\varepsilon}_n. \tag{5.6}$$

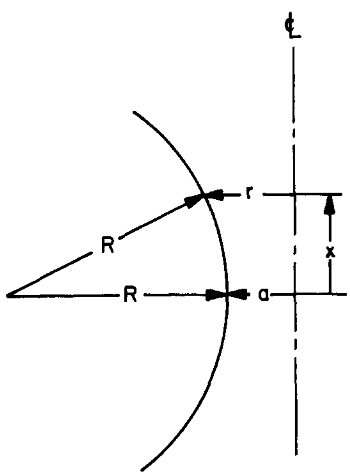

Figure 2. Assumed geometry of a neck. R is the radius of curvature of the osculating plane, a the minimum specimen radius and r the specimen radius at distance x from the minimum cross section.

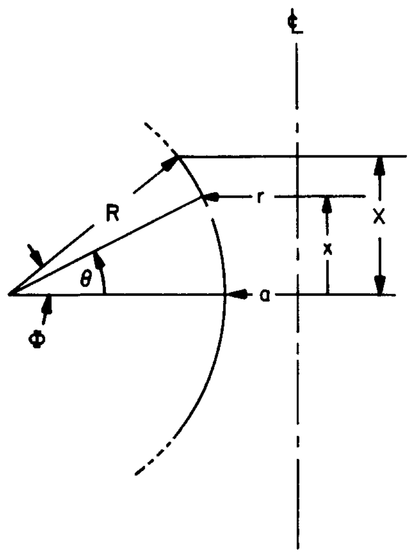

Figure 3. Assumed geometry of a neck. Coordinate x defines the angle θ and the extent X of the deforming region defines the angle Φ.

As the current cross sectional area of the neck is πa^2, equation (2.2) gives

$$\dot{\varepsilon}_n = -2\dot{a}/a. \tag{5.7}$$

Using (5.7), (5.6) and (5.2) in equation (5.5) we obtain

$$\dot{r} = -(a\dot{\varepsilon}_n/2)\{1 + R/a + 2kR^2/a^2 - (R/a)(1 + 2kR/a)[1 - (x/R)^2]^{-\frac{1}{2}}\}. \tag{5.8}$$

The cross sectional deformation stops at that value of x, say X, for which $\dot{r} = 0$. From (5.8) we have

$$(X/R)^2 = 1 - (R/a)^2(1 + 2kR/a)^2/(1 + R/a + 2kR^2/a^2)^2. \tag{5.9}$$

This limit of the deformation zone is more conveniently taken as the angle Φ shown in Fig. 3 with the obvious relation $\sin\Phi = (X/R)$ where X/R is obtained from (5.9). After some straightforward manipulations

$$\sin\Phi = [4k + 2a/R + a^2/R^2]^{\frac{1}{2}}/(1 + a/R + 2kR/a). \tag{5.10}$$

As the current cross sectional area at any position x within the deforming neck is πr^2, equation (2.2) gives

$$\dot{\varepsilon}(x, t) = -2\dot{r}/r. \tag{5.11}$$

Substitution from (5.8), (5.4) and (5.2) yields

$$\dot{\varepsilon}(x, t) = \frac{\dot{\varepsilon}_n(2k + a/R + a^2/R^2 - (2k + a/R)[1 - (x/R)^2]^{-\frac{1}{2}})}{k\varepsilon_n(1 + a/R - [1 - (x/R)^2]^{\frac{1}{2}})}. \tag{5.12}$$

The relative displacement rate of one face of the deforming zone with respect to the opposite face must equal the crosshead speed, S, of the testing machine. By symmetry:

$$S = 2\int_0^X \dot{\varepsilon}\,dx. \tag{5.13}$$

To perform the integration we introduce a new spatial variable θ as shown in Fig. 3, such that $\sin\theta = x/R$. Then $dx = R\cos\theta\,d\theta$, $[1-(x/R)^2]^{\frac{1}{2}} = \cos\theta$, so that using (5.12) (5.13) becomes

$$k\varepsilon_n S/2\dot{\varepsilon}_n = (2k + a/R + a^2/R^2)\int_0^{\Phi} \frac{R\cos\theta\,d\theta}{1 + a/R - \cos\theta} - (2k + a/R)\int_0^{\Phi} \frac{R\,d\theta}{1 + a/R - \cos\theta}. \tag{5.14}$$

Integration gives:

$$\begin{aligned} k\varepsilon_n S/2\dot{\varepsilon}_n = &-(2k + a/R + a^2/R^2)R\Phi \\ &+ [(2k + a/R + a^2/R^2)(1 + a/R) - (2k + a/R)] \\ &\times (2R/[(a/R)(2 + a/R)]^{\frac{1}{2}})\tan^{-1}\{[1 + 2R/a]^{\frac{1}{2}}\tan(\Phi/2)\}. \end{aligned} \tag{5.15}$$

Now Φ is specified by (5.10) and from (5.10) $\tan(\Phi/2)$ can be found by a simple trigonometric identity. Furthermore, from (5.2) and the relation $a = a_0\exp\{-\varepsilon_n/2\}$ we find that $R = (a_0/k\varepsilon_n)\exp\{-\varepsilon_n/2\}$. These relations and some simple algebra reduce (5.15) to the form

$$\begin{aligned} &(k\varepsilon_n/\dot{\varepsilon}_n)(S/L_0)(L_0/2a_0)\exp\{\varepsilon_n/2\} \\ &= \frac{2(2 + k\varepsilon_n + 2/\varepsilon_n)}{[1 + 2/k\varepsilon_n]^{\frac{1}{2}}}\tan^{-1}\left[\frac{\varepsilon_n(2 + k\varepsilon_n)}{4 + 2\varepsilon_n + k\varepsilon_n^2}\right]^{\frac{1}{2}} \\ &\quad - (1 + k\varepsilon_n + 2/\varepsilon_n)\sin^{-1}\left[\frac{k(4 + 2\varepsilon_n + k\varepsilon_n^2)}{(1 + k\varepsilon_n + 2/\varepsilon_n)^2}\right]^{\frac{1}{2}}. \end{aligned} \tag{5.16}$$

Here L_0 is the initial specimen length. Equation (5.16) provides the fundamental connection between nominal strain rate in the specimen, S/L_0, and maximum strain rate in the neck, $\dot{\varepsilon}_n$, in terms of the current neck strain, ε_n, the aspect ratio of the specimen, $2a_0/L_0$, and the constant k.

Phase II Elongation

For convenience we denote the right hand side of equation (5.16) by $g(\varepsilon_n)$. Then the Phase III strain rate at the minimum cross section is

$$\dot{\varepsilon}_n = k\varepsilon_n(S/L_0)(L_0/2a_0)\exp\{\varepsilon_n/2\}/g(\varepsilon_n) \tag{6.1}$$

whereas the Phase II strain rate, equation (3.5), is

$$\dot{\varepsilon} = (1/\nu)(S/L_0)\exp\{-\varepsilon_H\}(\exp\{\varepsilon - \varepsilon_H\} - 1 - \gamma(\varepsilon - \varepsilon_H) + \nu) \tag{6.2}$$

whenever $\nu \neq 0$. Ordinarily $\dot{\varepsilon}_n$ will exceed $\dot{\varepsilon}$ for strains very near ε_H. The transition from Phase II to Phase III will then occur when $\dot{\varepsilon}_n = \dot{\varepsilon}$. For $\nu = 0$ the transition occurs immediately upon reaching maximum load. Since $\dot{\varepsilon}$ from (6.2) becomes unbounded in this case it immediately exceeds $\dot{\varepsilon}_n$ from (6.1).

The Phase II to Phase III transition is governed entirely by the parameters, ε_H, $L_0/2a_0$, γ, ν and k. For any particular set of these parameters it is relatively simple to find the value of $\varepsilon_J = \varepsilon_n = \varepsilon$ for which $\dot{\varepsilon}_n = \dot{\varepsilon}$, by standard numerical techniques. Using this value as an upper limit of integration in equation (3.7) we can then compute the Phase II (post-uniform) elongation from

$$(S/L_0)(t_J - t_H) = \int_{\varepsilon_H}^{\varepsilon_J} \frac{\nu \exp\{\varepsilon_H\}\, d\varepsilon}{\exp\{\varepsilon - \varepsilon_H\} - 1 - \gamma(\varepsilon - \varepsilon_H) + \nu}. \tag{6.3}$$

This calculation was performed taking $\varepsilon_H = 0.2$, $L_0/2a_0 = 4.5$ (standard, half-inch diameter, round tension specimen) and $k = 0.75$ for several values of ν. For simplicity it was assumed that the Hart relation, $\gamma = 1 - \nu$ at maximum load, was valid.

Results of these calculations are shown in Fig. 4 and indicate a dramatic effect of strain rate sensitivity on Phase II elongation. For ν equal to 0 there is no Phase II elongation but for ν as small as 0.01 more than twenty percent post-uniform elongation is predicted by the

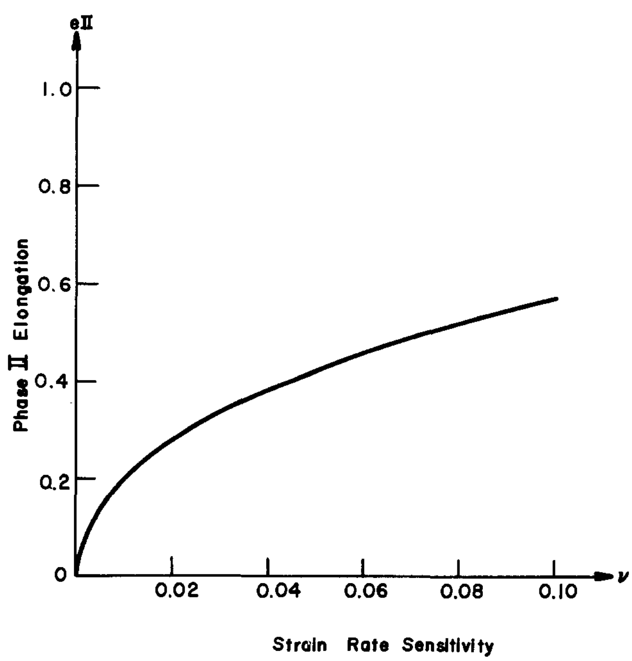

Figure 4. Post-uniform elongation versus strain rate sensitivity. For these calculations the strain at maximum load was taken as $\varepsilon_H = 0.2$, the specimen aspect ratio was taken as $L_0/2a_0 = 4.5$, and the approximation $\gamma = 1 - \nu$ was used.

analysis. So far as we are aware this is the strongest rate-sensitivity effect calculated from any extant models of the process.

We believe that a direct comparison of the results shown in Fig. 4 with experimental data such as that compiled by Ghosh (Fig. 4 of [16]) is not appropriate. The experimentally determined strain rate sensitivity parameter used by Ghosh is apparently that parameter denoted by Hart [17] as μ. That parameter is different from v, which is defined by equation (1.2), and usually considerably larger than v, as pointed out by Hart.

Load Drop

During Phase III the time is related to the neck strain ε_n by (4.7) which now has the form

$$(S/L_0)(t - t_J) = (2a_0/kL_0) \int_{\varepsilon_J}^{\varepsilon_n} d\varepsilon_n/[\varepsilon_n \exp\{\varepsilon_n/2\} g(\varepsilon_n)]. \tag{7.1}$$

The load ratio given by (4.13) becomes

$$P/P_H = [1 + \gamma(\varepsilon_n - \varepsilon_H) + (vkL_0/2a_0)\exp\{\varepsilon_n/2 - \varepsilon_H\}\varepsilon_n/g(\varepsilon_n)]\exp\{\varepsilon_H - \varepsilon_n\}. \tag{7.2}$$

For the same values of the parameters used in the calculations for Fig. 4 load drops were calculated following the onset of necking. The results are shown as plots of load ratio versus nominal strain in Fig. 5. The dashed curve for nominal strains up to $e_H = \exp\{\varepsilon_H\} - 1$ indicates an unspecified response during Phase I deformation. Clearly, there should be a smoother transitional behavior between Phases II and III which would make the overall description of the deformation somewhat more precise. Nevertheless, we believe that the

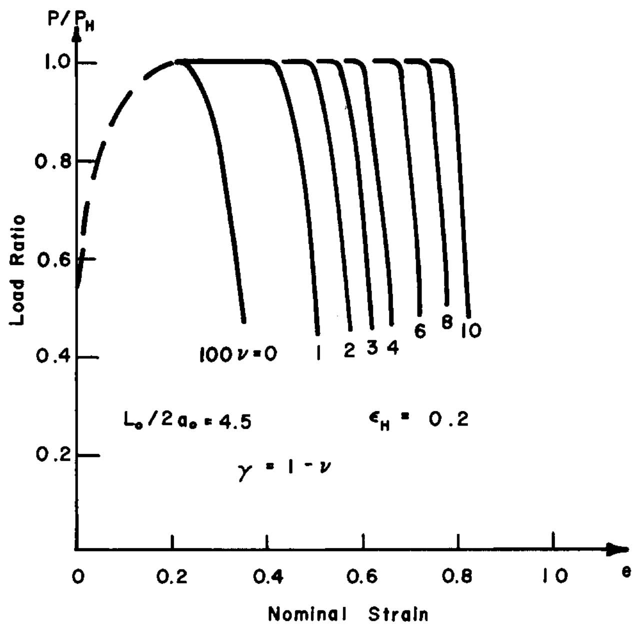

Figure 5. Nondimensionalized load versus extension curves for materials of different strain rate sensitivities. The shape of the dashed curve to $\varepsilon = \varepsilon_H$ depends upon the variations of γ and v during Phase I of the deformation.

present description is surprisingly accurate considering the simplicity of the underlying calculations.

Neck Profiles

At any time during Phase III, the portion of the neck that is actually straining is described by equation (5.2) as simply having a constant radius of curvature. However, this curvature changes with strain and those cross sections that have stopped straining also contribute to the shape of the specimen near the neck. To compute this overall shape consider a cross section in the neck that stops straining at $t = \tau$. From equations (5.4) and (5.9), after some algebraic simplifications and the use of (5.2), the radius of this cross section can be shown to be given by

$$r/a_0 = [1 + 1/k\varepsilon^* - [k(4 + 2\varepsilon^* + k\varepsilon^{*2})]^{\frac{1}{2}}/(1 + k\varepsilon^* + 2/\varepsilon^*)] \exp\{-\varepsilon^*/2\} \tag{8.1}$$

where $\varepsilon^* = \varepsilon_n(\tau)$.

For subsequent times, $t > \tau$, this cross section is embedded in one of the rigid portions of the specimen adjacent to the deforming neck. Since the neck is symmetrical the velocity of the critical cross section relative to each rigid portion of the specimen is $S/2$. Consequently, the position of the cross section under consideration, relative to the critical cross section, is

$$x = X^* + (t - \tau)S/2 \tag{8.2}$$

where $X^* = X(\tau)$. From (5.9) and some straightforward algebra:

$$X^* = (a_0/k\varepsilon^*) \exp\{-\varepsilon^*/2\}[k(4 + 2\varepsilon^* + k\varepsilon^{*2})]^{\frac{1}{2}}/(1 + k\varepsilon^* + 2/\varepsilon^*). \tag{8.3}$$

Thus the profile of the entire region centered at the neck becomes

$$r/a_0 = \begin{cases} \{1 + k\varepsilon_n - [1 - (xk\varepsilon_n/a_0)^2 \exp\{\varepsilon_n\}]^{\frac{1}{2}}\}/k\varepsilon_n \exp\{\varepsilon_n/2\}, & |x| \le X(t), \\ \{1 + 1/k\varepsilon^* - [k(4 + 2\varepsilon^{*2})]^{\frac{1}{2}}/(1 + k\varepsilon^* + 2/\varepsilon^*)\} \exp\{-\varepsilon^*/2\}, & |x| > X(t). \end{cases} \tag{8.4}$$

Here for $|x| > X(t)$ the connection between $\varepsilon^* < \varepsilon_n$ and x is through equation (8.2) taking account of (8.3).

Numerical calculations based upon the above equations gave the neck profiles shown in Fig. 6 at different stages of the Phase III deformation. Here, specimen radius is plotted vs axial position, both normalized with respect to the original radius of the bar. The vertical lines indicate the extent, X, of the deforming region at each stage. Although, the deforming region itself is always represented by a circular arc this geometry, in a natural way, leads to a change in sign of the curvature outside the deforming region. Thus, the neck profiles of Fig. 6 seem to be reasonably accurate representations of experimentally determined profiles.

An estimate of the incipient neck size can be made from (8.3) by letting ε^* reduce towards ε_H. For small values of ε^* the dominant term under the square root is $4k$, while that in the denominator is $2/\varepsilon^*$. Thus, $X^* \approx (a_0/k\varepsilon^*) \exp\{-\varepsilon^*/2\} 2k^{\frac{1}{2}}/(2/\varepsilon^*)$; or

$$X_J^* \approx (a_0/k^{\frac{1}{2}}) \exp\{-\varepsilon^*/2\} = a_J^*/k^{\frac{1}{2}} \tag{8.5}$$

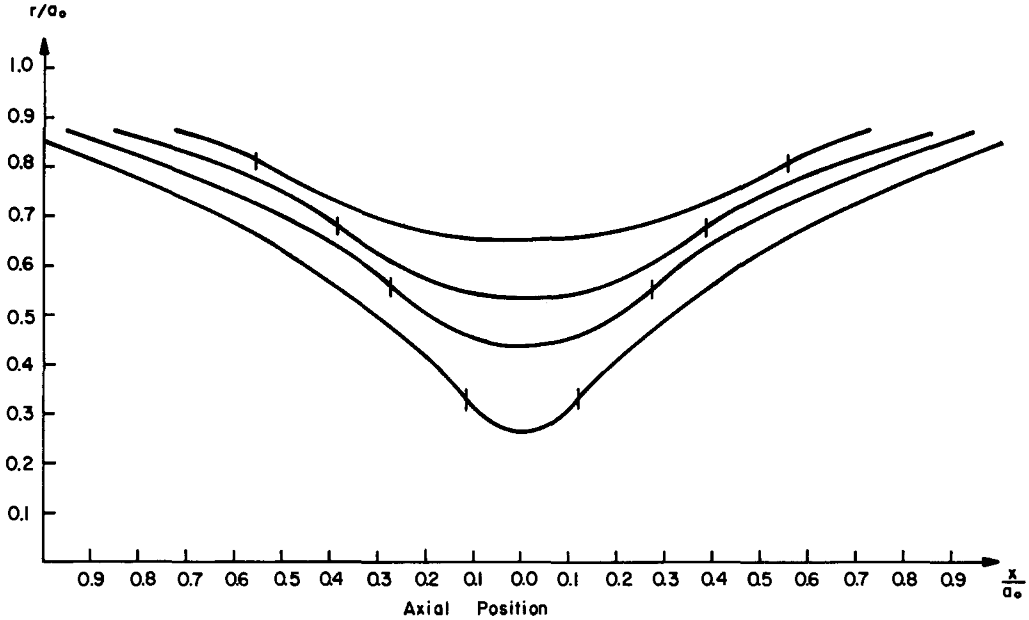

Figure 6. Neck profiles calculated at different stages of deformation. For these calculations the strain rate sensitivity parameter was taken as $\nu = 0.01$ and other parameters are the same as in Fig. 5. The vertical bars indicate the extent of the deforming region (X) at the different stages of deformation.

which shows that the neck initially forms over a specimen length, $2X_f^*$, approximately equal to the current specimen diameter (times a numerical factor of 1.15).

7. Discussion

The foregoing deformation analysis is quite general in the sense that it is not restricted to small variations in specimen cross sectional area. The analysis of Phase I indicates that the maximum load criterion, equation (2.12), contains an additional term not included in previous analyses.

The analyses of Phases II and III are independent of the crosshead speed of the testing machine, so long as it is constant. Hutchinson [8, 9] noted a similar result. However, the material can respond differently to different testing speeds through its Phase I behaviour. Thus, both the stress and strain at maximum load (as well as the stress, strain relation up to maximum load) could be influenced by crosshead speed.

The analysis of Phase II indicates that as the strain rate sensitivity increases, a considerable delay in necking can occur. The magnitude of this effect seems to be greater than predicted by previous analyses.

8. Conclusions

The present analysis realistically approximates: (1) Load, extension curves; (2) Post-uniform elongation; (3) Incipient neck size; and (4) Neck profiles; for both rate-sensitive and rate-insensitive materials.

Acknowledgements

This work was supported by the Air Force Office of Scientific Research through grant no. AFOSR-77-3379 to the University of Kentucky. The authors are also grateful to Dr. E. W. Hart for stimulating discussions and encouragement.

REFERENCES

[1] A. Considere, Mémoire sur l'emploi du fer et de l'acier dans les constructions, *Annales des Ponts et Chaussees*, Vol. 9 (1885) 574–775.
[2] W. A. Backofen, I. R. Turner and D. H. Avery, Superplasticity in an Al–Zn alloy, *Transactions of the A.S.M.*, Vol. 57 (1964) 980–990.
[3] E. W. Hart, Theory of the tensile test, *Acta Metallurgica*, Vol. 15 (1967) 351–355.
[4] J. D. Campbell, Plastic instability in rate-dependent materials, *Journal of the Mechanics and Physics of Solids*, Vol. 15 (1967) 359–370.
[5] J. J. Jonas, R. A. Holt and C. E. Coleman, Plastic stability in tension and compression, *Acta Metallurgica*, Vol. 24 (1976) 911–918.
[6] J. J. Jonas and B. Baudelet, Effect of crack and cavity generation on tensile stability, *Acta Metallurgica*, Vol. 25 (1977) 43–50.
[7] A. S. Argon, Stability of plastic deformation, Chapter 7 of *The Inhomogeneity of Plastic Deformation*, A.S.M., Metals Park, Ohio (1973) 161–189.
[8] J. W. Hutchinson and H. Obrecht, Tensile instabilities in strain-rate dependent materials, *Fracture 1977*, D.M.R., Taplin, Ed., University of Waterloo Press, Waterloo, Ontario, Vol. 1 (1977) 101–116.
[9] J. W. Hutchinson and K. W. Neale, Influence of strain-rate sensitivity on necking under uniaxial tension, *Acta Metallurgica*, Vol. 25 (1977) 839–846.
[10] A. K. Ghosh, A numerical analysis of the tension test for sheet metals, *Metallurgical Transactions A*, Vol. 8A (1977) 1221–1232.
[11] A. K. Ghosh, Tensile instability and necking in materials with strain hardening and strain-rate hardening, *Acta Metallurgica*, Vol. 25 (1977) 1413–1424.
[12] E. W. Hart, Constitutive relations for the nonelastic deformation of metals, *Journal of Engineering Materials and Technology*, Transactions of the A.S.M.E., Vol. 98, Ser. H (1976) 193–202.
[13] I. G. Dondik, Equation of the neck profile of tensile specimens, *Strength of Materials* (Problemy Prochnosti translated from Russian Vol. 3, 1971, No. 8, pp. 54–56) translation published in 1972 as Vol. 3 (1971) 937–940.
[14] A. S. Argon, J. Im and A. Needleman, Distribution of plastic strain and negative pressure in necked steel and copper bars, *Metallurgical Transactions A*, Vol. 6A (1975) 815–824.
[15] P. W. Bridgman, *Studies in large plastic flow and fracture*, McGraw-Hill, New York, 1952.
[16] A. K. Ghosh, The influence of strain hardening and strain-rate sensitivity on sheet metal forming, *Journal of Engineering Materials and Technology*, Transactions of the A.S.M.E., Vol. 99, Ser. H (1977) 264–274.
[17] E. W. Hart, Theories of "superplastic" behavior, *General Electric Research and Development Center Report No. 69-C-029*, dated December 1968.